Excited state switching in rhenium(I) bipyridyl complexes with donor- donor and donor-acceptor substituents

Joshua J. Sutton[1,2], Dan Preston[1,2], Philipp Traber[3], Johannes Steinmetzer[3], Xue Wu[4], Surajit Kayal[4], Xue Z Sun[4], James D. Crowley[1,2], Michael W. George[4,5*], Stephan Kupfer[3*], Keith C. Gordon[1,2*]

[1] Department of Chemistry, University of Otago, Dunedin, New Zealand, 9016

[2] MacDiarmid Institute for Advanced Materials and Nanotechnology, New Zealand

[3] Institute for Physical Chemistry, Friedrich Schiller University Jena, Helmholtzweg 4, 07743 Jena, Germany

[4] School of Chemistry, University of Nottingham, Nottingham NG7 2RD, United Kingdom

[5] Department of Chemical and Environmental Engineering, University of Nottingham Ningbo China, 199 Taikang East Road, Ningbo 315100 China

KEYWORDS Resonance Raman spectroscopy, Donor Acceptor, Transient Emission, Time-resolved IR, Transient Absorption, scalar relativistic quantum chemistry, benzothiadiazole, triphenylamine, rhenium.

ABSTRACT: The optical properties of two $Re(CO)_3(bpy)Cl$ complexes in which the bpy is substituted with two donor (triphenylamine, TPA, $ReTPA_2$) as well as both donor (TPA) and acceptor (benzothiadiazole, BTD, ReTPA-BTD) groups are presented. For $ReTPA_2$ the absorption spectra show intense intraligand charge-transfer (ILCT) bands at 460 nm with small solvatochromic behavior, for ReTPA-BTD the ILCT transitions are weaker. These are assigned as TPA → bpy transitions as supported by resonance Raman data and TDDFT calculations. The excited state spectroscopy shows the presence of two emissive states for both complexes. The intensity of these emission signals is modulated by solvent. Time-resolved infrared spectroscopy definitively assigns the excited states present in CH_2Cl_2 to be MLCT in nature and in MeCN the excited states are ILCT in nature. This switching with solvent may be explained through calculations in which the access to states is controlled by spin-orbit coupling and this is sufficiently different in the two solvents to select out each of the charge-transfer states.

Introduction

Inorganic donor-acceptor (DA) systems, based around diimine ligands have been extensively studied due to being electronically and structurally diverse, with interesting and complex behaviours.[1-5] This can be achieved by modification of the ligand or metal center, with metals such as Ru(II),[6] Os(II),[6-7] Re(I),[8-9]and Cu(I)[9] having been utilized. One system of particular interest is $Re(CO)_3(NN)X$, where NN is a diimine ligand such as 2,2' bipyridine (bpy),[8-11] 1,10-phenanthroline (phen)[12-17] or dipyrido[3,2-a:2',3'-c]phenazine (dppz)[18-20].

Through substitution of the diimine ligand, the energy of the lowest energy excited state can be modified. Worl *et al.*[8] demonstrated structural changes could be used to tune the excited state by changing the electron withdrawing nature of 4,4'-substituted bipyridyl ligands. This resulted in a systematic tuning of the energy of the lowest energy state and lifetime of the MLCT (metal-to-ligand charge-transfer) state. Similar results have been reported for phen based systems.[21] The use of more structurally and electronically complex ligands, such as dppz, accesses a range of new states. By using dppz as the diimine ligand, it is possible to populate MLCT states in which the photoexcited electron resides on phen or phenazine (phz) based molecular orbitals, a ligand centered state may also be populated.[22-25] The interplay between these states, coupled with the fact the $MLCT_{phen}$ state is emissive, while the $MLCT_{phz}$ state is dark results in dppz complexes showing a "light-switch"

behaviour, which can be exploited for sensing the chemical environment the complex is in.[22, 26]

It is possible to alter the electronic structure of metal polypyridyl complexes further by the introduction of ligands which are themselves active chromophores or electroactive. This merging of inorganic and organic chromophores is recognized as a useful way to imbue materials with new optical properties.[27] This can tune the MLCT state, or add new ligand based states such as ligand centered (LC) or intra-ligand charge transfer (ILCT), with the ligand based states existing with some degree of communication with the MLCT states. One example of this is the work of Castellano *et al.* who demonstrated that by attaching a naphthalene-dicarboximide or pyrenyl based group to a phen diimine ligand for Re(I), Ir(II) and Ru(II) complexes. The lifetime of the MLCT state of the Re compound was over 500 μs, at room temperature in deaerated tetrahydrofuran, due to coupling between the ^{3}MLCT and naphthalene-dicarboximide or pyrenyl based ^{3}LC. This resulted in an oscillation ("ping-ponging") between the two types of triplet states, ultimately increasing the lifetime of the excited population.[13, 28-31] For the $Re(CO)_3(NN)X$ systems modification of the ancillary ligand (X) can also be used to tune the electronic behaviour of the complexes. It has been shown that by attaching an ethene or ethyne linked donor to a pyridine ancillary ligand resulted in an ancillary based, dark, intraligand state, which could interact with the lowest energy MLCT state.[32-43]

Another example of this is given by Kitamura *et al.*, they showed that the appending of triarylborane electronic acceptor off phen or bpy diimine ligands significantly perturbs the electronic nature of the system.[44-48] This is due to the interaction between the MLCT and ligand based π_{aryl}-p(B) CT states, which resulted in increased MLCT absorbance and lifetimes. Kitamura *et al,* studied bpy diimine ligands with triphenylborane (TPB) units on either the 4 or 4 and 4' positions.[45, 49] It was found in shifting from the mono- to the di-substituted systems resulted in increased conjugation and lowered the energy of the MLCT transition, with a red-shifted of 2200 cm^{-1}. The lowering of energy of the MLCT state combined with its more extensive conjugation can affect the excited state lifetime in two ways; firstly the reduced energy gap decreases the lifetime as shown by Worl *et al.*, the effect of the increased conjugation or greater delocalization of the excited state can increase the lifetime by reducing the non-radiative decay pathways as shown by Treadway *et al.*[50] In this case the balance of factors leads to an increased lifetime (140 ns) relative to the parent species $Re(CO)_3(bpy)Cl$ (90 ns).[49]

Recently Wang *et al.*[51] constructed ligands in which the TPA donors and $BMes_2$ acceptor units were incorporated into copper complexes. The lowest energy absorbance of these complexes was found to be dominated by ligand characteristic. The lowest energy transition was found, via computational modelling, to be predominately ILCT in nature, with only slight MLCT contribution.[51-52] The emissive propertied showed greater variation upon complexation, with a 6000 cm^{-1} redshift in the emission maximum and two order of magnitude decrease in the lifetime at 77 K.

In a series of studies on donor acceptor ligands incorporating TPA and dppz it was found that the photophysics was dominated by ILCT excited states. The rationale for this was that the acceptor MO was based on the phenazine MO of the dppz which is electronically disconnected from the metal centre.[18-19, 25, 53] Additional studies on 1,10-phenanthroline based ligands with appended TPA units also showed ILCT excited states playing a dominant role in the optical properties and photochemistry; again the metals played a peripheral role.[12, 54]

In an attempt to better understand the interactions between appended donor (and acceptor units) on metal-to-ligand charge-transfer chromophores we have used ethyne linkers with appended donor (TPA) and acceptor benzothiadiazole (BTD) groups on Re(bpy) systems. These complexes build on earlier studies using ethylene linkers.[9] The complexes were studied using a range of electronic and spectroscopic techniques, including transient emission and absorbance spectroscopies, resonance Raman spectroscopy and time-resolved IR and Raman spectroscopies, with the experimental data complemented by quantum chemical simulations performed at the density functional (DFT) and time-dependent DFT (TDDFT) level of theory including scalar relativistic effects.

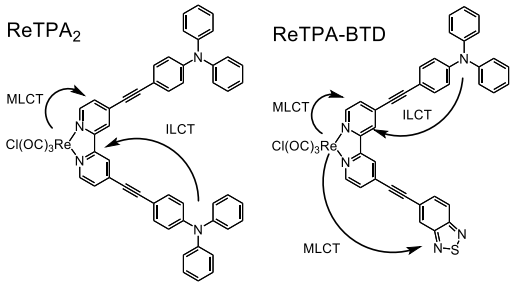

Figure 1: Pair of D-A complexes studied in this work. Arrows indicate key potential CT transitions.

Table 1: TDDFT predicted lowest energy transitions (S_1 to S_7) for $ReTPA_2$ as calculated in CH_2Cl_2 and MeCN.

$ReTPA_2$: CH_2Cl_2						
State	Transition	Weight / %	ΔE / eV	λ / nm	f	λ_{exp} / nm
S_1	$\pi_{TPA}(218) \rightarrow \pi^*_{bpy}(219)$ (ILCT)	54	2.82	440	0.4920	466
	$d_{Re}(216) \rightarrow \pi^*_{bpy}(219)$ (MLCT)	34				
S_2	$\pi_{TPA}(217) \rightarrow \pi^*_{bpy}(219)$ (ILCT)	68	2.90	428	1.1759	448
	$d_{Re}(215) \rightarrow \pi^*_{bpy}(219)$ (MLCT)	20				
S_3	$d_{Re}(216) \rightarrow \pi^*_{bpy}(219)$ (MLCT)	62	2.99	414	0.2952	-
	$\pi_{TPA}(218) \rightarrow \pi^*_{bpy}(219)$ (ILCT)	24				
S_4	$d_{Re}(215) \rightarrow \pi^*_{bpy}(219)$ (MLCT)	75	3.16	392	0.1328	-
	$\pi_{TPA}(217) \rightarrow \pi^*_{bpy}(219)$ (ILCT)	15				
S_5	$\pi_{TPA}(217) \rightarrow \pi^*_{bpy}(220)$ (ILCT)	65	3.49	355	0.3370	368
	$\pi_{TPA}(218) \rightarrow \pi^*_{bpy}(219)$ (ILCT)	13				
S_6	$d_{Re}(214) \rightarrow \pi^*_{bpy}(219)$ (MLCT)	96	3.49	355	0.0039	-
S_7	$\pi_{TPA}(218) \rightarrow \pi^*_{bpy}(220)$ (ILCT)	69	3.52	352	0.6809	362
	$\pi_{TPA}(217) \rightarrow \pi^*_{bpy}(219)$ (ILCT)	3				
$ReTPA_2$: MeCN						
State	Transition	Weight / %	ΔE / eV	λ / nm	f	λ_{exp} / nm
S_1	$\pi_{TPA}(218) \rightarrow \pi^*_{bpy}(219)$ (ILCT)	68	2.85	436	0.6174	446
	$d_{Re}(216) \rightarrow \pi^*_{bpy}(219)$ (MLCT)	20				
S_2	$\pi_{TPA}(217) \rightarrow \pi^*_{bpy}(219)$ (ILCT)	77	2.93	424	1.2019	437
	$d_{Re}(215) \rightarrow \pi^*_{bpy}(219)$ (MLCT)	13				
S_3	$d_{Re}(216) \rightarrow \pi^*_{bpy}(219)$ (MLCT)	76	3.04	407	0.1639	-
	$\pi_{TPA}(218) \rightarrow \pi^*_{bpy}(219)$ (ILCT)	14				
S_4	$d_{Re}(215) \rightarrow \pi^*_{bpy}(219)$ (MLCT)	82	3.22	385	0.0517	-
	$\pi_{TPA}(217) \rightarrow \pi^*_{bpy}(219)$ (ILCT)	10				
S_5	$\pi_{TPA}(217) \rightarrow \pi^*_{bpy}(220)$ (ILCT)	69	3.50	354	0.3471	359
	$\pi_{TPA}(218) \rightarrow \pi^*_{bpy}(219)$ (ILCT)	13				
S_6	$\pi_{TPA}(218) \rightarrow \pi^*_{bpy}(220)$ (ILCT)	73	3.53	351	0.6892	350
	$\pi_{TPA}(217) \rightarrow \pi^*_{bpy}(219)$ (ILCT)	8				
S_7	$d_{Re}(214) \rightarrow \pi^*_{bpy}(219)$ (MLCT)	95	3.55	350	0.0121	-

Electronic spectroscopy

The absorption spectra of the complexes were recorded in a variety of solvents (Figure 2). Both complexes exhibited two distinct transitions in the spectral region of interest, at about 350 and 440 nm. Across the range of solvents studied the absorbance maximum of the lowest energy transition shifted about 130 cm^{-1}. For ReTPA-BTD the lowest energy transition showed about half extinction coefficient of $ReTPA_2$. This, combined with the small variation in absorbance energy between the complexes suggest the lowest energy is similar in both complexes and has a large degree of ILCT TPA→BTD character. The dependence of the extinction coefficient of the lowest energy transition on the number of donor units is consistent with what has been reported for similar systems.[55-56]

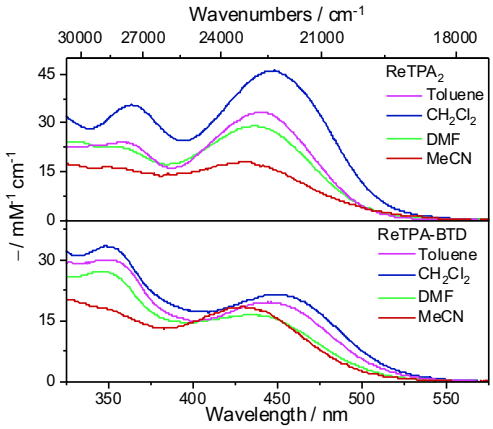

Figure 2: Electronic absorbance spectra for $ReTPA_2$ and ReTPA-BTD in a range of solvents.

A more detailed insight into the nature of the chromophores may be afforded by the use of TDDFT calculations. Quantum chemical simulations at the TDDFT level of theory have been performed for both complexes including implicit solvent effects for MeCN and CH_2Cl_2, respectively (details of these methods are given in Section 5 of the ESI). The predicted excited state properties are in good agreement with the experimental data and, thus allow assignment of the electronic transitions. In case of $ReTPA_2$ these data are presented in Table 1. This shows that intense transitions are predicted at about 450 nm, as observed and these are attributed to bright states (S_1 and S_2) that are involve electron density changes at both the potential donor sites (the $Re_{d\pi}$ and the TPA_{π}) however they are predominantly ILCT in nature. At higher energy states that are predominantly MLCT in character are predicted (S_3 and S_4) and at 350 nm additional ILCT transitions – with different orbital parentage from the S_1 and S_2 states may be seen (S_5 and S_6). The calculations show broadly the same behaviour whether suing the CH_2Cl_2 solvent field or that for MeCN – consistent with the experimental data.

Resonance Raman Spectroscopy

Resonance Raman spectroscopy (RRS) may be used to experimentally evaluate the nature of chromophores in the electronic spectra.[32, 57-63] For these compounds the RRS spectra were collected from 355 to 491 nm in both CH_2Cl_2 (Figure 3) and MeCN (Figures S15 and S16). From the experimental RRS data and computational modelling the nature of the lowest energy transitions may be assigned. The TDDFT (Tables 1, S1-S6) simulations provide further insight into the nature of the electronic transitions, which can be used to support the analysis of the RRS. The agreement of the simulated and the experimental spectra (Figure 3) demonstrates the accuracy of the applied computational protocol to elucidate the excited state properties for the present Re(I) complexes, allowing for confidence when interpreting the TDDFT data.

The resonance Raman data for $ReTPA_2$ are shown in Figure 3a. The pattern of band enhancement changes on going from 355 nm excitation to 491 nm. For $ReTPA_2$ the band enhancement pattern alters between $\lambda_{exc.}$ = 355 nm and 375 nm with the ν_{234} vibrational mode losing intensity relative to ν_{240}. Eigenvectors for all key modes discussed here can be found in Tables S11. The enhancement pattern changes again on going to longer wavelengths with a subtle increase in the relative intensity of ν_{165} with redder excitation. The simulations comprise contributions from excitations into the states S_1 to S_4 in the blue part of the visible region and into S_5 and S_6 in the UV region (see section 5.1 in the ESI for details) and allow to reproduce, and thus to assign, the experimentally observed band patterns with respect to the excitation wavelength.

All transitions show enhancement of a mixture of TPA and bpy modes, along with the C≡C modes (ν_{248} and ν_{249}) stretching mode and slight enhancement of the metal carbonyl symmetric stretching mode (ν_{246}). These data are consistent with the simulated RRS data (also shown in Figure 3 and detailed in Tables S7 to S10). It is possible to use the relative enhancements of differing modes as proxies of orbital involvement in the various transitions that are present. For example for $ReTPA_2$ ν_{248} is enhanced by ILCT transitions from π_{TPA} to π^*_{bpy}. However, the higher energy transitions, S_3 and S_4, show greatest enhancement of a bpy based mode (ν_{228}) and, relatively, less enhancement of the C≡C modes (ν_{248} and ν_{249}). This suggests that the higher energy transition have more bpy ππ* or MLCT character than the ILCT dominated lower energy transitions. The increased $MLCT_{bpy}$ character is seen in the increased enhancement of the metal carbonyl stretching mode in the calculations.

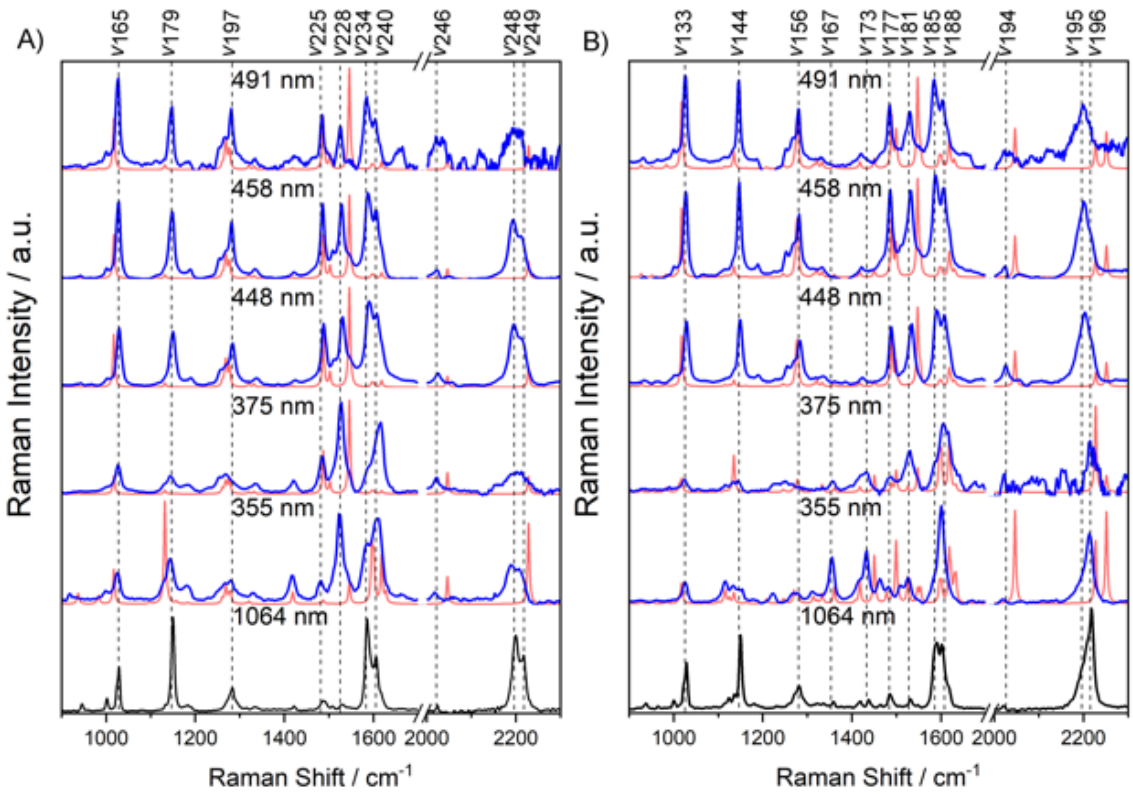

Figure 3: Resonance Raman spectra for $ReTPA_2$ (A) and ReTPA-BTD (B) in CH_2Cl_2 (10^{-3} mol L^{-1}) at the excitation wavelengths listed. Eigenvectors for all labeled can be found in Table S11.

For ReTPA-BTD again four unique transitions are observed, the three lowest energy, lying above 400 nm and at 375 nm are similar to those observed for $ReTPA_2$ and can be assigned to the mixed $\pi_{TPA}\pi^*_{BTD}$ / $\pi_{TPA}\pi^*_{bpy}$ excitation (S_1) as well as to the $MLCT_{bpy}$ excitations S_2 and S_3. The enhancement pattern, particularly of ν_{195} over ν_{196} (Figures S15 and S16), suggests that the predicted $\pi_{TPA}\pi^*_{BTD}$ contribution has little effect on the spectral signature. Another transition, resonant at 355 nm, shows enhancement of both the BTD moiety (ν_{156} over ν_{167}; see Figures S15 and S16) and the metal carbonyl (ν_{194}) and this is consistent with a $MLCT_{BTD}$ transition. As with the lower energy transitions this assignment is supported by computational modeling revealing the semi-bright and bright states S_5 and S_6 (both in MeCN and in CH_2Cl_2), see Table S4. In addition enhancement of the bpy to BTD C≡C (ν_{195}) over the bpy to TPA C≡C (ν_{196}) further supports this assignment.

Emission Spectroscopy

The electronic emission spectra for these complexes were found to be solvent sensitive (Figure 4). Each complex showed two distinct emission bands, termed low energy (LE) and high energy (HE). In solvents with a low polarity LE (~650 nm) and HE (~420-500 nm) emission were observed, with the LE emission showing greater relative intensity. This LE emission is consistent with that reported for the comparable copper complexes.[51] The HE emission profile is comprised of two peaks. In $ReTPA_2$ these occur at 425 and 500 nm, while in ReTPA-BTD they occur at 420 and 445 nm. In more polar solvents, the LE emission loses intensity. For $ReTPA_2$ this drop off is near complete, however for ReTPA-BTD a weak peak at ~650 nm is still present. Due to the energy of the HE emission it can be surmised that emission band is inaccessible up initial S_1 photoexcitation and most likely arises from higher energy MLCT states (S_3 or S_4 in $ReTPA_2$ and S_5 or S_6 in ReTPA-BTD, as calculated by TDDFT (Tables 1 and S4 and Figures S23 and S24)). This is supported by the excitation profile of the HE emission peak (Figure S13).

The strong change in the emission as a response to solvent suggests that the solvents are influencing the complex.

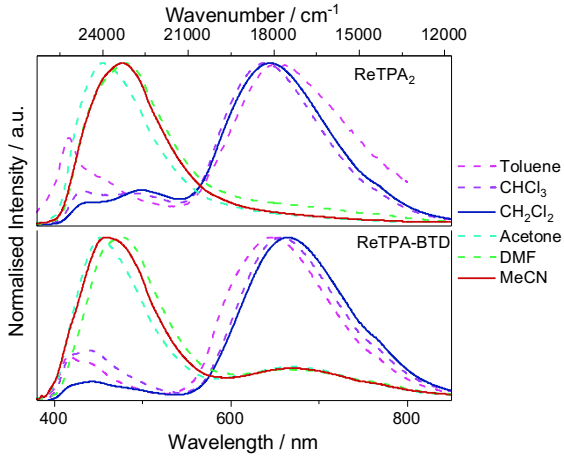

Figure 4: Steady state emission spectra for $ReTPA_2$ and ReTPA-BTD in a range of different solvents.

Transient Absorption and Emission Spectroscopies

The excited state dynamics were first examined using transient emission (TE) spectroscopy. Spectra were recorded in CH_2Cl_2 and MeCN for both complexes. In CH_2Cl_2 the HE emission of both complexes was found to be short-lived τ <6 ns, consistent with a singlet state (Figure S18). The LE transition however was found to be longer -lived τ ~200 ns for $ReTPA_2$ and τ ~100 ns for ReTPA-BTD (Figure S19). The existence of dual emission has also been observed by Liu *et. al*[64] for Pt complexes with similar D-A-D bpy based ligands, with similar TPA based donors.

In MeCN a short singlet emission was observed, with a lifetime of <6 ns in both complexes. This is consistent with the high energy emission in CH_2Cl_2, suggesting that between CH_2Cl_2 and MeCN we see a loss of the low energy triplet emission.

In addition to TE, transient absorbance (TA) was used to examine the behaviour of each complex in CH_2Cl_2 and MeCN, respectively. Between the solvents both complexes showed consistent variations in their respective TA spectra (Figure 5). In CH_2Cl_2 the excited state absorbance is consistently red shifted relative to that of MeCN and significantly greater intensity is observed at ~800 nm. Variations between $ReTPA_2$ and ReTPA-BTD were observed. The peaks in ReTPA-BTD were consistently broader than those in $ReTPA_2$. Furthermore, $ReTPA_2$ showed an excited state absorption at 350 nm, not seen in ReTPA-BTD. The presence of the strong absorbance at 780 nm is consistent with the $TPA^{\bullet+}$ species,[7, 18, 53, 65] while the strong absorption at 390 nm is consistent with $bpy^{\bullet-}$.[66-67]

When the lifetimes of the TA where compared between CH_2Cl_2 and MeCN (Figure S20) further insight into the variations in the excited state nature was observed. In CH_2Cl_2 lifetimes consistent with those observed in the TE were recorded, 190 (± 20) ns for $ReTPA_2$ and 100 (± 20) ns for ReTPA-BTD. However, while the TE for both complexes in MeCN showed only singlet emission a long-lived excited state was observed in the TA. In $ReTPA_2$ a lifetime of 140 (± 20) ns was recorded, while for ReTPA-BTD the lifetime was 80 (± 20) ns. These results mean that in CH_2Cl_2 there is a long-lived emissive state, but in MeCN the nature of the excited state has been modified to result in a 'dark' excited state.

The TA and TE properties of $ReTPA_2$ differ from those for the alkene bridge analogue. While the steady state properties are similar with regards to the energy of the transitions the lifetimes vary significantly. The alkene bridge analogue shows a single emissive state with a τ < 10 ns and a 'dark' state (τ ~ 600 ns) in CH_2Cl_2.[9]

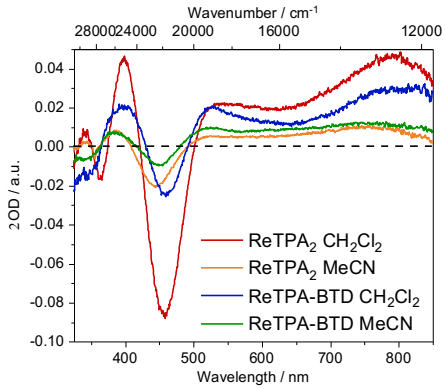

Figure 5: TA spectra for both complexes in MeCN and CH_2Cl_2.

Time Resolved IR Spectroscopy

In order to gain further insight into the nature of the excited states and how it varies with respect to solvent time-resolved IR (TRIR) spectra of $ReTPA_2$ and ReTPA-BTD were collected in CH_2Cl_2 and MeCN. Figure 6 shows the TRIR spectra for both complexes obtained 1 ps after irradiation in CH_2Cl_2 – evidently, ν(C=O) peaks are bleached and transients are produced with bands shifted up relative the ground state. This shift of the C=O stretching modes to higher wavenumbers in indicative of an MLCT transition.[20, 68-69] As time delay of the TRIR is increased from 1 to 50 ps, the transient bands narrow and shift to

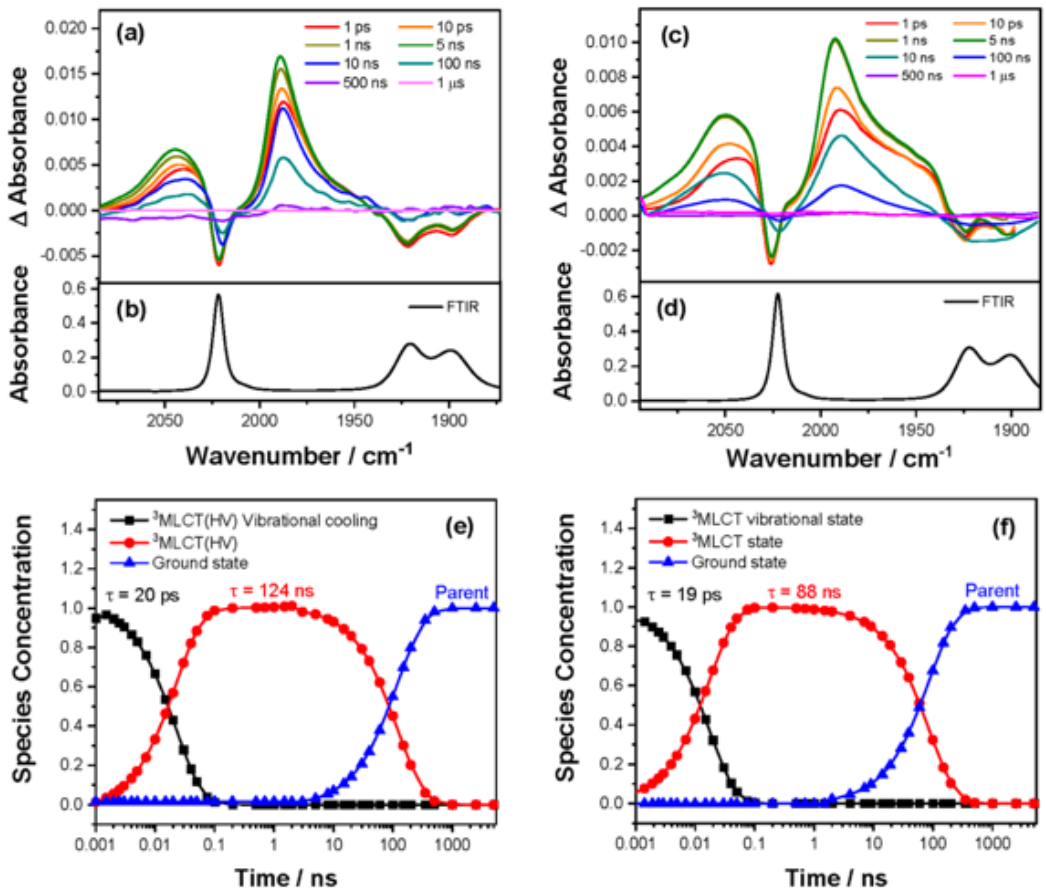

Figure 6: TRIR spectra obtained following irradiation of (a) $ReTPA_2$ and (b) ReTPA-BTD in CH_2Cl_2 together with the decay profiles obtained from global fitting from these data for (c) $ReTPA_2$ and (d) ReTPA-BTD.

slightly higher wavenumber ($ReTPA_2$: 2045 and 1990 cm^{-1} and ReTPA-BTD: 2050 and 1993 cm^{-1}) which is consistent with vibrational cooling from the initial excited state being generated in a vibrationally excited state similar that observed in *fac*-Re(bpy)CO_3Cl.[70] Thus, this MLCT transition can be assigned as a vibrational state: ^{3}MLCT. Figure 6 also shows the kinetic profile obtained from the global analysis of these TRIR data with initial decay from a vibrationally excited state of ca. 20 ps for both complexes followed by a decay back to the respective parent (τ = 125 ns ($ReTPA_2$) and τ = 90 ns (ReTPA-BTD)). Overall, these two transitions decayed on the nanosecond timescale can be assigned as the lowest-lying electronic ^{3}MLCT state in each Re complex.

In MeCN however significantly different results were observed. Figure 7 shows the TRIR spectra for both complexes obtained 1 ps after irradiation in MeCN and it is clear that following that parent ν(C=O) peaks are bleached and transients are produced with bands mainly shifted down relative the ground state (see Figure 7). The TRIR spectra reveal that the photophysics of $ReTPA_2$ and ReTPA-BTD is more complex in MeCN compared to those obtained in CH_2Cl_2 and there appear to be ν(C=O) bands shifted up as well as down relative to the parent bands. The interpretation is aided by global analysis of these data and the TRIR spectra shows the presence of at least five species that contribute to the evolving TRIR spectra for both complexes. Initially the parent bands are bleached, and two transients are produced with largely ILCT character initially in a vibrationally excited state. These species behavior differently following vibrational cooling. The first shorter lived state (state 1) shows ν(CO) bands shifted to higher wavenumber (lower intensity) with the presence of

bands shifted to higher wavenumber bands being more noticeable in the TRIR spectra of ReTPA-BTD but for both complexes the TRIR kinetics obtained from the ν(CO) bands to high and low wavenumber decay show the same decay kinetics (see ESI) and state 1 is tentatively assigned to a mixed MLCT/ILCT state. State 1 decays back to the ground state and global analysis shows state 1 ReTPA-BTD (τ = 34 ps) decays slightly quicker than in vase of $ReTPA_2$ (τ = 57 ps). The longer lived ILCT state (state 2) decays partially to reform the parent and to form another transient also with ICLT character. This process is tentatively assigned to a ^{1}ILCT state decay to the parent and also forming ^{3}ILCT, which subsequently decays back to the parent on the 50-100 ns timescale. The kinetics for conversion of ^{1}ILCT → ^{3}ICLT are slightly quicker for ReTPA-BTD (τ = 400 ps) compared to $ReTPA_2$ (τ = 1-2 ns). These lifetimes are consistent with the 'dark' state observed in the TA.

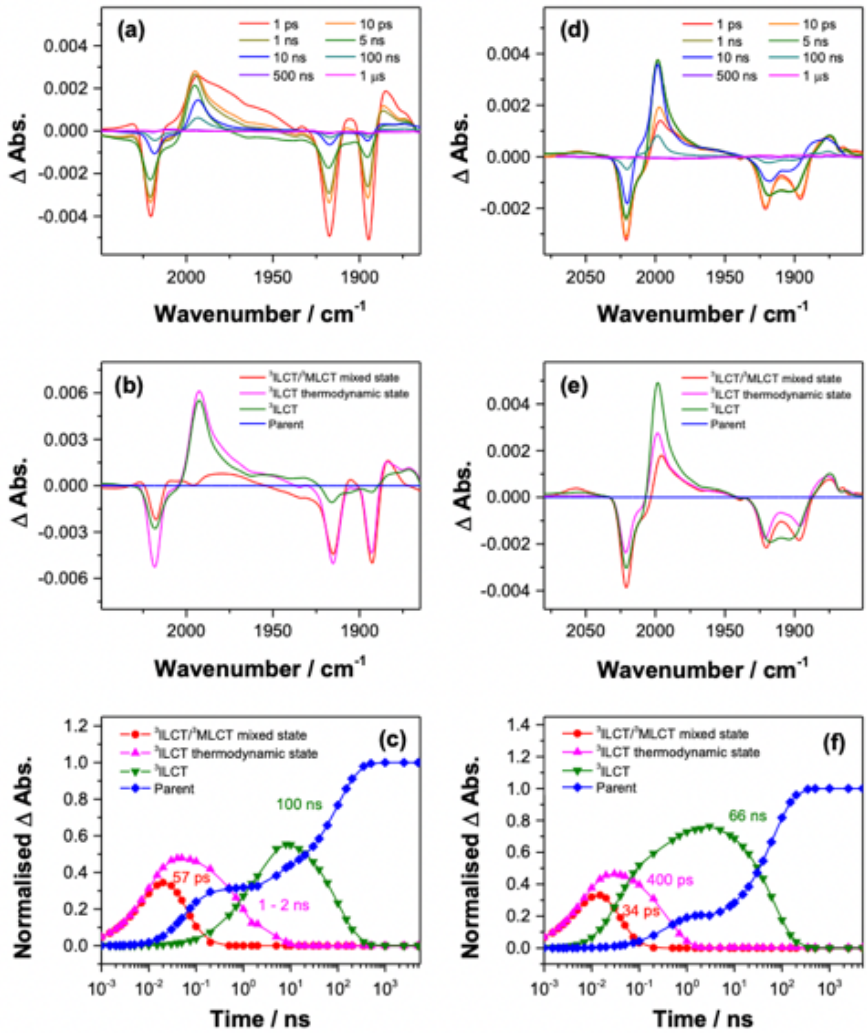

Figure 7: TRIR spectra and spectra and decay profiles obtained from global fitting obtained following irradiation of $ReTPA_2$ ((a) TRIR spectra, (b) global fit loading and (c) global fit decay profiles) and ReTPA-BTD ((d) TRIR spectra, (e) global fit loading and (f) global fit decay profiles) in CH_2Cl_2.

The combination of time-resolved and steady state techniques allowed to provide detailed insight into the excited state nature and dynamics of the complexes. From the RRS it can be determined that the immediately populated state is identical in nature in both complexes in both solvents. This stated shows a mix of ILCT(TPA-bpy) and MLCT(Re-bpy) in nature. From the TA, TE and TRIR data it can be seen that the long-lived triplet state varies in nature, depending on solvent. In CH_2Cl_2 a long-lived emissive state is observed, which was assigned as ^{3}MLCT in nature. However, in MeCN the long-lived state is dark in nature and, from TRIR, is identified as being ^{3}ILCT.

The tuning of the lowest accessible triplet state between MLCT and ILCT as a function of solvent environment is atypical and has important ramification for the overall excited state dynamics for the $Re(CO)_3(NN)X$ complexes as accessing a MLCT or ILCT state with while significant impacts on the quantum yield and ability to tune the energy of the said state.

Computational Modelling

To evaluate the unexpected highly solvent-dependent nature of the excited relaxation pathways on a molecular level, we performed (scalar relativistic) TDDFT simulations to address i) the intersystem crossing (ISC) at the Franck-Condon (FC) point based on the spin-orbit couplings (SOCs) among the initially bright excited states in the vicinity of the excitation wavelength of 355 nm and the energetically close triplet states and ii) the nature of the emissive state. Insight into the singlet-triplet population transfer was obtained at the SR-ZORA-TDDFT level of theory, whereas the SOC among the spin-free singlet and triplet states allowed for the prediction of the nature of the initially populated triplet state in the FC region. In agreement with the simulation for previously investigated structurally similar $Re(CO)_3(NN)X$ complexes,[12] an efficient SOC is exclusively possible between ^{1}MLCT and ^{3}MLCT states, which feature typically pronounced SOCs ranging from 200 to 600 cm^{-1}. On the other hand, couplings among ^{1}ILCT and ^{3}MLCT states are mostly predicted between 0 and 100 cm^{-1}. This general picture is obtained in both MeCN and CH_2Cl_2 and is not surprising as the ^{1}ILCT excitation does not involve the Re center. Therefore, independent of the oscillator strength for the excitation into the ^{1}MLCT states, population transfer to the triplet manifold is exclusively possible via a ^{1}MLCT/^{3}MLCT gateway. Surprisingly, the nature of the gateway highly depends on the solvent but not on the substitution pattern of the investigated Re(I) systems. In MeCN, $ReTPA_2$ and ReTPA-BTD show a pronounced SOC of 614 and 395 cm^{-1}, respectively, from the S_3 ^{1}MLCT state ($ReTPA_2$: at 389 nm; ReTPA-BTD: at 387 nm) to the T_{12} ^{3}MLCT state ($ReTPA_2$: at 342 nm; ReTPA-BTD: at 348 nm), which features the unpaired electrons in the d_{xy} and the π^*_{bpy} orbitals (Tables S14 and S22). However, in the less polar CH_2Cl_2 several efficient spin-orbit interactions are estimated between the ^{1}MLCT state S_3 ($ReTPA_2$: at 399 nm; ReTPA-BTD: at 395 nm) and the energetically close ^{3}MLCT states, while the respective SOCs are with 133-434 cm^{-1} considerably smaller. In addition, neither of these coupled ^{3}MLCT states in CH_2Cl_2 is of $d_{xy}\pi^*_{bpy}$ nature. Therefore, the solvent polarity allows to control the ^{1}MLCT/^{3}MLCT gateways as well as the subsequent excited states relaxation pathways.

The solvent-dependent energetic landscape of the low-lying triplet states were investigated by DFT and TDDFT simulations for $ReTPA_2$ and ReTPA-BTD. The lowest ^{3}ILCT and ^{3}MLCT states (Franck-Condon region) in $ReTPA_2$ were fully relaxed to gain insight into possible emissive channels. In MeCN, the ^{3}ILCT Franck-Condon state (T_1) is predicted at an energy of 2.20 eV and undergoes merely a slight stabilization of 0.05 eV upon equilibration, while the ^{3}MLCT (T_3) is stabilized by ~0.17 eV along the ^{3}ILCT relaxation coordinate (Figure 8). Such difference in excited state stabilization is not surprising, as the geometry differences between the FC region and ILCT structures are commonly small, while MLCT state are more sensitive to structural alterations. In a similar fashion, the ^{3}MLCT state, (2.83 eV, FC region), is stabilized by almost 0.6 eV upon equilibration along the ^{3}MLCT relaxation coordinate, while the energy of the ^{3}ILCT state is increased to 2.56 eV. Thus, both the ^{3}ILCT as well as the ^{3}MLCT states are predicted to be the lowest triplet states within their respective equilibrium structures, i.e. at 2.15 (^{3}ILCT) and 2.24 eV (^{3}MLCT) (Figure 8). In the less polar CH_2Cl_2, the ^{3}ILCT (2.19 eV, FC region) is stabilized more efficiently to 2.00 and 2.15 eV within the ^{3}ILCT and ^{3}MLCT structures, respectively. The energy of the ^{3}MLCT, 2.78 eV at the FC point and at 2.61 and 2.40 eV within the ^{3}ILCT and the ^{3}MLCT minima, is less effected by CH_2Cl_2. Therefore, the nature of the lowest triplet state is not affected by in the less polar solvent, in contrast, the pronounced ^{3}MLCT stabilization in the polar MeCN alters the decay pathway, allowing access of the ^{3}ILCT state. For ReTPA-BTD the general picture with respect to the solvent-dependent stabilization along the respective ^{3}ILCT vs. ^{3}MLCT relaxation pathways is in line with the results obtained for $ReTPA_2$. However, for the D-A-A complex, a TPA→BTD ^{3}IL state is predicted by TDDFT to be always the most stable triplet state, *i.e.* within its ^{3}IL equilibrium but also within the ^{3}ILCT and the ^{3}MLCT equilibrium structure. More details regarding the excited state relaxation pathways are collected in the supporting information.

The combination of scalar-relativist simulations on the SOCs within the FC region as well as the excited state optimizations addressing the nature of the emissive state form an energetic perspective allows to draw a consistent picture: The polarity of the solvent highly affects the ^{1}MLCT/^{3}MLCT gateway, especially the character of the accessible ^{3}MLCT state(s) but also the size of the SOCs. Consequentially, different relaxation pathways are observed both within MeCN and CH_2Cl_2, while the solvent affects both complexes in a similar fashion. From an energetic point of view, the lowest lying state is ^{3}ILCT – or of ^{3}IL for ReTPA-BTD – in nature for both solvent fields. However minimal spin-orbit coupling between the singlet and ^{3}ILCT states (Tables S16, S20, S24 and S28) prevents direct population of the ^{3}ILCT, meaning in CH_2Cl_2 the excited state decay occurs from

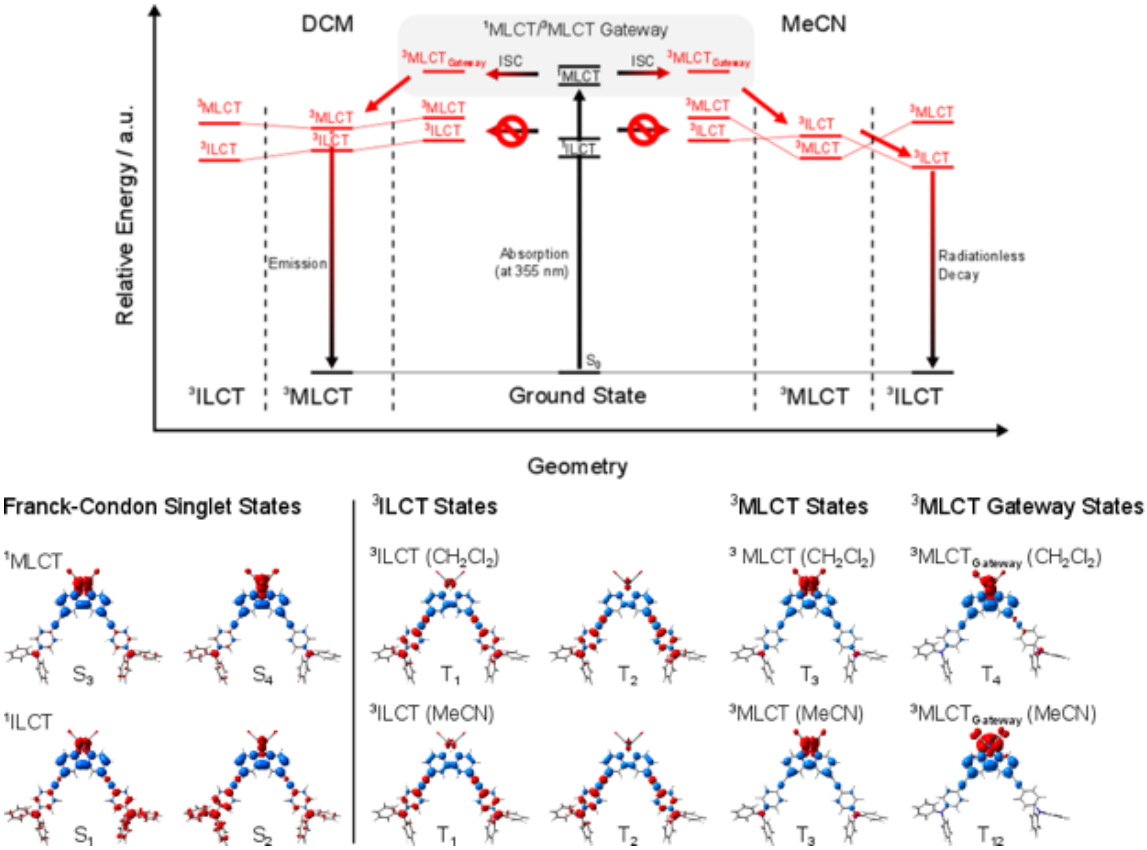

Figure 8: Simplified overview of the various excited states, relative energies and transitions for $ReTPA_2$ in CH_2Cl_2 and MeCN. See ESI for details of calculated energy of various states.

the ^{3}MLCT state. However, in MeCN the energy of the ^{3}MLCT is lowered such that the ^{3}MLCT PES intersects with the ^{3}ILCT PES, this allows for the ^{3}ILCT state to be populated via internal conversion for the initially accessible ^{3}MLCT states. This computational data agrees with the overall picture from the experimental data, which is summarized in Figure 8.

Conclusion

The excited state nature and dynamics of a pair of new D-A-D and D-A-A Re complexes were explored. From the combination of TRIR, TA and TE it was determined that the lowest accessible triplet state was varied between an emissive ^{3}MLCT and dark ^{3}ILCT with changing solvent environment. This variation in behaviour was linked to the dramatic alteration of the singlet-triplet population transfer as shown by scalar-relativistic quantum chemical simulation. The simulations clearly show that the polarity of the solvent highly affects both: the electronic nature as well as the SOCs of the triplet accessible by the ^{1}MLCT/^{3}MLCT gateway. In the case

of solvents with a low polarity the excited state gets trapped in a ^{3}MLCT state and must decay back to the ground state from there. However, in more polar solvents the optimized ^{3}MLCT geometry is lowered in energy to create an intersection point with the ^{3}ILCT manifold, allowing access to the lower energy ^{3}ILCT. This has a series of implications for material design; it clearly demonstrated the importance of having accessible MLCT states in order to get significant population of triplet states; and the structural relaxation in the excited state controls the final accessible state. The dependence of the accessible excited states on the solvent highlights the need to take a high-level caution when trying to understand or predict how a material will perform in different device or environment than initially studied. It is also interesting to note that the ground state properties do not provide any insight into the solvent switching of the excited states – further complicating predictions.

General

All physical measurements were carried out in spectroscopic grade solvents as supplied. Spectral data was analyzed using the combination of GRAMS A/I (ThermoFisher, USA), Origin Pro 2018 (Origin Lab Corporation, USA), Flurocale (Edinburgh Instruments, UK) and Spectragryph 1.2 (Dr. Friedrich Menges, Germany).

Synthesis

Synthetic details can be found in the ESI

Physical Measurements

Steady state emission, excitation emission maps and the fluorescence lifetimes on a FS5 (Edinburgh Instruments, UK), using specifications as previously reported.[12, 62, 71] Transient absorption data was collected using a LP920K (Edinburgh Instruments, UK), with the setup details reported previously.[12, 53-54, 62, 71] FT-Raman spectra were recorded in the solid state using a Bruker MultiRam (Bruker, USA), with a 1064 nm Nd:YAG excitation source and a D418T germanium diode detector. Resonance Raman spectra were collect using a 135° illumination backscattering setup as previously described.[12, 72-73] Details of the TRIR experimental setup have be previously reported.

Computational Modelling

Computational details can be found in the ESI

ASSOCIATED CONTENT

Supporting Information. Synthetic detail, ligand emission, RRS in MeCN, key vibrational modes, TA and TE spectra and decay traces, TDDFT calculations, RRS calculations, TRIR spectra and global analysis of TRIR are provided in the supporting information. This material is available free of charge via the Internet at http://pubs.acs.org.

AUTHOR INFORMATION

Corresponding Author

Keith Gordon - keith.gordon@otago.ac.nz
Stephan Kupfer - stephan.kupfer@uni-jena.de
Michael George - mike.george@nottingham.ac.uk

Present Addresses

†If an author's address is different than the one given in the affiliation line, this information may be included here.

Author Contributions

All authors have given approval to the final version of the manuscript.

ACKNOWLEDGMENT

Support from the University of Otago, Friedrich Schiller University Jena, University of Nottingham and MacDiarmid Institute is gratefully acknowledged. All calculations were performed at the Universitätsrechenzentrum of the Friedrich Schiller University of Jena.

ABBREVIATIONS

RRS, resonance Raman spectroscopy; DFT, density functional theory; TDDFT, time-dependent density functional theory; TRIR, time-resolved infrared; BTD, benzothiadiazole; TPA, triphenylamine; BPY, bipyridine; MLCT, metal-to-ligand charge-transfer; ILCT, intraligand charge transfer; GS, ground state; ES, excited state; MeCN, acetonitrile; CH_2Cl_2, dichloromethane.

REFERENCES

1. Horvath, R.; Gordon, K. C., Understanding excited-state structure in metal polypyridyl complexes using resonance Raman excitation profiles, time-resolved resonance Raman spectroscopy and density functional theory. *Coord. Chem. Rev.,* **2010,** *254*, 2505-2518.
2. Lo, K. K.-W.; Zhang, K. Y.; Li, S. P.-Y., Recent Exploitation of Luminescent Rhenium(I) Tricarbonyl Polypyridine Complexes as Biomolecular and Cellular Probes. *Eur. J. Inorg. Chem.,* **2011,** *2011*, 3551-3568.
3. Lee, L. C.-C.; Leung, K.-K.; Lo, K. K.-W., Recent development of luminescent rhenium(i) tricarbonyl polypyridine complexes as cellular imaging reagents, anticancer drugs, and antibacterial agents. *Dalton Trans.* **2017,** *46*, 16357-16380.
4. Baba, A. I.; Shaw, J. R.; Simon, J. A.; Thummel, R. P.; Schmehl, R. H., The photophysical behavior of d6 complexes having nearly isoenergetic MLCT and ligand localized excited states. *Coord. Chem. Rev.,* **1998,** *171*, 43-59.

5. Stufkens, D. J.; Vlček, A., Ligand-dependent excited state behaviour of Re(I) and Ru(II) carbonyl–diimine complexes. *Coord. Chem. Rev.,* **1998,** *177*, 127-179.
6. van Slageren, J.; Hartl, F.; Stufkens, D. J.; Martino, D. M.; van Willigen, H., Changes in excited-state character of [M(L1)(L2)(CO)2(α-diimine)] (M=Ru, Os) induced by variation of L1 and L2. *Coord. Chem. Rev.,* **2000,** *208*, 309-320.
7. Hankache, J.; Wenger, O. S., Large Increase of the Lifetime of a Charge-Separated State in a Molecular Triad Induced by Hydrogen-Bonding Solvent. *Chem. Eur. J.* **2012,** *18*, 6443-6447.
8. Worl, L. A.; Duesing, R.; Chen, P.; Ciana, L. D.; Meyer, T. J., Photophysical properties of polypyridyl carbonyl complexes of rhenium(I). *J. Chem. Soc., Dalton Trans* **1991**, 849-858.
9. Horvath, R.; Fraser, M. G.; Cameron, S. A.; Blackman, A. G.; Wagner, P.; Officer, D. L.; Gordon, K. C., Synthesis, Characterization, and Photophysics of Oxadiazole- and Diphenylaniline-Substituted Re(I) and Cu(I) Complexes. *Inorg. Chem.* **2013,** *52*, 1304-1317.
10. Coe, B. J.; Foxon, S. P.; Pilkington, R. A.; Sánchez, S.; Whittaker, D.; Clays, K.; Van Steerteghem, N.; Brunschwig, B. S., Rhenium(I) Tricarbonyl Complexes with Peripheral N-Coordination Sites: A Foundation for Heterotrimetallic Nonlinear Optical Chromophores. *Organometallics* **2016,** *35*, 3014-3024.
11. Coe, B. J.; Foxon, S. P.; Pilkington, R. A.; Sánchez, S.; Whittaker, D.; Clays, K.; Depotter, G.; Brunschwig, B. S., Nonlinear Optical Chromophores with Two Ferrocenyl, Octamethylferrocenyl, or 4-(Diphenylamino)phenyl Groups Attached to Rhenium(I) or Zinc(II) Centers. *Organometallics* **2015,** *34*, 1701-1715.
12. Shillito, G. E.; Hall, T. B. J.; Preston, D.; Traber, P.; Wu, L.; Reynolds, K. E. A.; Horvath, R.; Sun, X. Z.; Lucas, N. T.; Crowley, J. D.; George, M. W.; Kupfer, S.; Gordon, K. C., Dramatic Alteration of 3ILCT Lifetimes Using Ancillary Ligands in [Re(L)(CO)3(phen-TPA)]n+ Complexes: An Integrated Spectroscopic and Theoretical Study. *J. Am. Chem. Soc.,* **2018,** *140*, 4534-4542.
13. Yarnell, J. E.; Deaton, J. C.; McCusker, C. E.; Castellano, F. N., Bidirectional "Ping-Pong" Energy Transfer and 3000-Fold Lifetime Enhancement in a Re(I) Charge Transfer Complex. *Inorg. Chem.,* **2011,** *50*, 7820-7830.
14. Pomestchenko, I. E.; Polyansky, D. E.; Castellano, F. N., Influence of a Gold(I)–Acetylide Subunit on the Photophysics of Re(Phen)(CO)3Cl. *Inorg. Chem.,* **2005,** *44*, 3412-3421.
15. Zipp, A. P.; Sacksteder, L.; Streich, J.; Cook, A.; Demas, J. N.; DeGraff, B. A., Luminescence of rhenium(I) complexes with highly sterically hindered .alpha.-diimine ligands. *Inorg. Chem.,* **1993,** *32*, 5629-5632.
16. Ko, C.-C.; Kwok, W.-M.; Yam, V. W.-W.; Phillips, D. L., Triplet MLCT Photosensitization of the Ring-Closing Reaction of Diarylethenes by Design and Synthesis of a Photochromic Rhenium(I) Complex of a Diarylethene-Containing 1,10-Phenanthroline Ligand. *Chem. Eur. J.* **2006,** *12*, 5840-5848.
17. Pu, Y.-J.; Harding, R. E.; Stevenson, S. G.; Namdas, E. B.; Tedeschi, C.; Markham, J. P. J.; Rummings, R. J.; Burn, P. L.; Samuel, I. D. W., Solution processable phosphorescent rhenium(i) dendrimers. *J. Mater. Chem.* **2007,** *17*, 4255-4264.
18. Larsen, C. B.; van der Salm, H.; Clark, C. A.; Elliott, A. B. S.; Fraser, M. G.; Horvath, R.; Lucas, N. T.; Sun, X.-Z.; George, M. W.; Gordon, K. C., Intraligand Charge-Transfer Excited States in Re(I) Complexes with Donor-Substituted Dipyridophenazine Ligands. *Inorg. Chem.,* **2014,** *53*, 1339-1354.
19. Larsen, C. B.; van der Salm, H.; Shillito, G. E.; Lucas, N. T.; Gordon, K. C., Tuning the Rainbow: Systematic Modulation of Donor–Acceptor Systems through Donor Substituents and Solvent. *Inorg. Chem.,* **2016,** *55*, 8446-8458.
20. van der Salm, H.; Fraser, M. G.; Horvath, R.; Cameron, S. A.; Barnsley, J. E.; Sun, X.-Z.; George, M. W.; Gordon, K. C., Re(I) Complexes of Substituted dppz: A Computational and Spectroscopic Study. *Inorg. Chem.,* **2014,** *53*, 3126-3140.
21. Wrighton, M.; Morse, D. L., Nature of the lowest excited state in tricarbonylchloro-1,10-phenanthrolinerhenium(I) and related complexes. *J. Am. Chem. Soc.,* **1974,** *96*, 998-1003.
22. Brennaman, M. K.; Meyer, T. J.; Papanikolas, J. M., [Ru(bpy)2dppz]2+ Light-Switch Mechanism in Protic Solvents as Studied through Temperature-Dependent Lifetime Measurements. *J. Phys. Chem. A* **2004,** *108*, 9938-9944.
23. Fees, J.; Kaim, W.; Moscherosch, M.; Matheis, W.; Klima, J.; Krejcik, M.; Zalis, S., Electronic structure of the "molecular light switch" bis(bipyridine)dipyrido[3,2-a:2',3'-c]phenazineruthenium(2+). Cyclic voltammetric, UV/visible and EPR/ENDOR study of multiply reduced complexes and ligands. *Inorg. Chem.,* **1993,** *32*, 166-174.
24. Stoeffler, H. D.; Thornton, N. B.; Temkin, S. L.; Schanze, K. S., Unusual Photophysics of a Rhenium(I) Dipyridophenazine Complex in Homogeneous Solution and Bound to DNA. *J. Am. Chem. Soc.,* **1995,** *117*, 7119-7128.
25. van der Salm, H.; Larsen, C. B.; McLay, J. R. W.; Fraser, M. G.; Lucas, N. T.; Gordon, K. C., Stretching the phenazine MO in dppz: the effect of phenyl and phenyl-ethynyl groups on the photophysics

of Re(I) dppz complexes. *Dalton Trans.***2014,** *43*, 17775-17785.
26. Jenkins, Y.; Friedman, A. E.; Turro, N. J.; Barton, J. K., Characterization of dipyridophenazine complexes of ruthenium(II): The light switch effect as a function of nucleic acid sequence and conformation. *Biochemistry* **1992,** *31*, 10809-10816.
27. Castellano, F. N., Altering Molecular Photophysics by Merging Organic and Inorganic Chromophores. *Acc. Chem. Res* **2015,** *48*, 828-839.
28. Yarnell, J. E.; McCusker, C. E.; Leeds, A. J.; Breaux, J. M.; Castellano, F. N., Exposing the Excited-State Equilibrium in an IrIII Bichromophore: A Combined Time Resolved Spectroscopy and Computational Study. *Eur. J. Inorg. Chem.,* **2016,** *2016*, 1808-1818.
29. McCusker, C. E.; Chakraborty, A.; Castellano, F. N., Excited State Equilibrium Induced Lifetime Extension in a Dinuclear Platinum(II) Complex. *J. Phys. Chem. A* **2014,** *118*, 10391-10399.
30. Tyson, D. S.; Henbest, K. B.; Bialecki, J.; Castellano, F. N., Excited State Processes in Ruthenium(II)/Pyrenyl Complexes Displaying Extended Lifetimes. *J. Phys. Chem. A* **2001,** *105*, 8154-8161.
31. Tyson, D. S.; Luman, C. R.; Zhou, X.; Castellano, F. N., New Ru(II) Chromophores with Extended Excited-State Lifetimes. *Inorg. Chem.,* **2001,** *40*, 4063-4071.
32. Cleland, D. M.; Irwin, G.; Wagner, P.; Officer, D. L.; Gordon, K. C., Linker Conjugation Effects in Rhenium(I) Bifunctional Hole-Transport/Emitter Molecules. *Chem. Eur. J.* **2009,** *15*, 3682-3690.
33. Constable, E. C.; Housecroft, C. E.; Kocik, M. K.; Neuburger, M.; Schaffner, S.; Zampese, J. A., Structural and photophysical properties of (phosphane)gold(I)-decorated 4,4'-diethynyl-2,2'-bipyridine ligands. *Eur. J. Inorg. Chem.* **2009**, 4710-4717.
34. Garakyaraghi, S.; McCusker, C. E.; Khan, S.; Koutnik, P.; Bui, A. T.; Castellano, F. N., Enhancing the Visible-Light Absorption and Excited-State Properties of Cu(I) MLCT Excited States. *Inorg. Chem.* **2018,** *57*, 2296-2307.
35. Glazer, E. C.; Magde, D.; Tor, Y., Ruthenium Complexes That Break the Rules: Structural Features Controlling Dual Emission. *J. Am. Chem. Soc.* **2007,** *129*, 8544-8551.
36. Johansson, P. G.; Zhang, Y.; Meyer, G. J.; Galoppini, E., Homoleptic "Star" Ru(II) Polypyridyl Complexes: Shielded Chromophores to Study Charge-Transfer at the Sensitizer-TiO2 Interface. *Inorg. Chem.* **2013,** *52*, 7947-7957.
37. Kisel, K. S.; Eskelinen, T.; Zafar, W.; Solomatina, A. I.; Hirva, P.; Grachava, E. V.; Tunik, S. P.; Koshevoy, I. O., Chromophore-Functionalized Phenanthro-diimine Ligands and Their Re(I) Complexes. *Inorg. Chem.,* **2018,** *57*, 6349-6361.
38. Klemens, T.; Switlicka-Olszewska, A.; Machura, B.; Grucela, M.; Janeczek, H.; Schab-Balcerzak, E.; Szlapa, A.; Kula, S.; Krompiec, S.; Smolarek, K.; Kowalska, D.; Mackowski, S.; Erfurt, K.; Lodowski, P., Synthesis, photophysical properties and application in organic light emitting devices of rhenium(I) carbonyls incorporating functionalized 2,2 ':6 ',2 "-terpyridines. *Rsc Advances* **2016,** *6*, 56335-56352.
39. Li, Y.; Liu, R.; Badaeva, E.; Kilina, S.; Sun, W., Long-Lived π-Shape Platinum(II) Diimine Complexes Bearing 7-Benzothiazolylfluoren-2-yl Motif on the Bipyridine and Acetylide Ligands: Admixing π,π* and Charge-Transfer Configurations. *J. Phys. Chem. C* **2013,** *117*, 5908-5918.
40. So, G. K.-M.; Cheng, G.; Wang, J.; Chang, X.; Kwok, C.-C.; Zhang, H.; Che, C.-M., Efficient Color-Tunable Copper(I) Complexes and Their Applications in Solution-Processed Organic Light-Emitting Diodes. *Chem. - Asian J.* **2017,** *12*, 1490-1498.
41. Stengel, I.; Strassert, C. A.; Plummer, E. A.; Chien, C.-H.; De Cola, L.; Baeuerle, P., Postfunctionalization of Luminescent Bipyridine PtII Bisacetylides by Click Chemistry. *Eur. J. Inorg. Chem.* **2012,** *2012*, 1795-1809.
42. Yu, T.; Tsang, D. P. K.; Au, V. K. M.; Lam, W. H.; Chan, M. Y.; Yam, V. W. W., Deep Red to Near-Infrared Emitting Rhenium(I) Complexes: Synthesis, Characterization, Electrochemistry, Photophysics, and Electroluminescence Studies. *Chem. Eur. J.* **2013,** *19*, 13418-13427.
43. Miller, M. T.; Karpishin, T. B., Phenylethynyl Substituent Effects on the Photophysics and Electrochemistry of [Cu(dpp)2]+ (dpp = 2,9-Diphenyl-1,10-phenanthroline). *Inorg. Chem.* **1999,** *38*, 5246-5249.
44. Ito, A.; Kang, Y.; Saito, S.; Sakuda, E.; Kitamura, N., Photophysical and Photoredox Characteristics of a Novel Tricarbonyl Rhenium(I) Complex Having an Arylborane-Appended Aromatic Diimine Ligand. *Inorg. Chem.,* **2012,** *51*, 7722-7732.
45. Nakagawa, A.; Sakuda, E.; Ito, A.; Kitamura, N., Remarkably Intense Emission from Ruthenium(II) Complexes with Multiple Borane Centers. *Inorg. Chem.* **2015,** *54*, 10287-10295.
46. Nakagawa, A.; Ito, A.; Sakuda, E.; Fujii, S.; Kitamura, N., Bright and Long-Lived Emission from a Starburst-Type Arylborane-Appended Polypyridyl Ruthenium(II) Complex. *Eur. J. Inorg. Chem.* **2017,** *2017*, 3794-3798.
47. Sakuda, E.; Ando, Y.; Ito, A.; Kitamura, N., Long-Lived and Temperature-Independent Emission from a Novel Ruthenium(II) Complex Having an Arylborane Charge-Transfer Unit. *Inorg. Chem.,* **2011,** *50*, 1603-1613.

48. Sakuda, E.; Matsumoto, C.; Ando, Y.; Ito, A.; Mochida, K.; Nakagawa, A.; Kitamura, N., Dual Emissions from Ruthenium(II) Complexes Having 4-Arylethynyl-1,10-phenanthroline at Low Temperature. *Inorg. Chem.,* **2015,** *54*, 3245-3252.
49. Kang, Y.; Ito, A.; Sakuda, E.; Kitamura, N., Characteristic Spectroscopic and Photophysical Properties of Tricarbonyl Rhenium(I) Complexes Having Multiple Arylborane Charge Transfer Units. *Bull. Chem. Soc. Jpn.* **2017,** *90*, 574-585.
50. Treadway, J. A.; Loeb, B.; Lopez, R.; Anderson, P. A.; Keene, F. R.; Meyer, T. J., Effect of Delocalization and Rigidity in the Acceptor Ligand on MLCT Excited-State Decay. *Inorg. Chem.,* **1996,** *35*, 2242-2246.
51. Zhao, Z.; Yin, X.; Peng, T.; Wang, N.; Wang, S., Triarylboron/Triarylamine-Functionalized 2,2′-Bipyridine Ligands and Their Copper(I) Complexes. *Inorg. Chem.,* **2020,** *59*, 7426–7434.
52. Risi, G.; Becker, M.; Housecroft, C. E.; Constable, E. C., Are Alkynyl Spacers in Ancillary Ligands in Heteroleptic Bis(diimine)copper(I) Dyes Beneficial for Dye Performance in Dye-Sensitized Solar Cells? *Molecules* **2020,** *25*.
53. Shillito, G. E.; Larsen, C. B.; McLay, J. R. W.; Lucas, N. T.; Gordon, K. C., Effect of Bridge Alteration on Ground- and Excited-State Properties of Ruthenium(II) Complexes with Electron-Donor-Substituted Dipyrido[3,2-a:2′,3′-c]phenazine Ligands. *Inorg. Chem.,* **2016,** *55*, 11170-11184.
54. Shillito, G. E.; Preston, D.; Traber, P.; Steinmetzer, J.; McAdam, C. J.; Crowley, J. D.; Wagner, P.; Kupfer, S.; Gordon, K. C., Excited-State Switching Frustrates the Tuning of Properties in Triphenylamine-Donor-Ligand Rhenium(I) and Platinum(II) Complexes. *Inorg. Chem.,* **2020,** *59*, 6736-6746.
55. Larsen, C. B.; Barnsley, J. E.; Salm, H. v. d.; Fraser, M. G.; Lucas, N. T.; Gordon, K. C., Synthesis and Optical Properties of Unsymmetrically Substituted Triarylamine Hexaazatrinaphthalenes. *Eur. J. Org. Chem.* **2017,** *2017*, 2432-2440.
56. Barnsley, J. E.; Lomax, B. A.; McLay, J. R. W.; Larsen, C. B.; Lucas, N. T.; Gordon, K. C., Flicking the Switch on Donor–Acceptor Interactions in Hexaazatrinaphthalene Dyes: A Spectroscopic and Computational Study. *ChemPhotoChem* **2017,** *1*, 432-441.
57. Horvath, R.; Huff, G. S.; Gordon, K. C.; George, M. W., Probing the excited state nature of coordination complexes with blended organic and inorganic chromophores using vibrational spectroscopy. *Coord. Chem. Rev.,* **2016,** *325*, 41-58.
58. Walsh, P. J.; Gordon, K. C.; Lundin, N. J.; Blackman, A. G., Photoexcitation in Cu(I) and Re(I) Complexes Containing Substituted Dipyrido[3,2-a:2',3'-c]phenazine: A Spectroscopic and Density Functional Theoretical Study. *J. Phys. Chem. A* **2005,** *109*, 5933-5942.
59. Lind, S. J.; Gordon, K. C.; Gambhir, S.; Officer, D. L., A spectroscopic and DFT study of thiophene-substituted metalloporphyrins as dye-sensitized solar cell dyes. *Phys. Chem. Chem. Phys.* **2009,** *11*, 5598-5607.
60. Wächtler, M.; Guthmuller, J.; González, L.; Dietzek, B., Analysis and characterization of coordination compounds by resonance Raman spectroscopy. *Coord. Chem. Rev.,* **2012,** *256*, 1479-1508.
61. Myers, A. B., Resonance Raman Intensity Analysis of Excited-State Dynamics. *Acc. Chem. Res* **1997,** *30*, 519-527.
62. Mapley, J. I.; Hayes, P.; Officer, D. L.; Wagner, P.; Gordon, K. C., Investigation of Ferrocene Linkers in β-Substituted Porphyrins. *J. Phys. Chem. A* **2020,** *124*, 5513-5522.
63. Mapley, J. I.; Ross, D. A. W.; McAdam, C. J.; Gordon, K. C.; Crowley, J. D., Triphenylamine-substituted 2-pyridyl-1,2,3-triazole copper(I) complexes: an experimental and computational investigation. *J. Coord. Chem.***2019,** *72*, 1378-1394.
64. Liu, R.; Li, Y.; Chang, J.; Waclawik, E. R.; Sun, W., Pt(II) Bipyridyl Complexes Bearing Substituted Fluorenyl Motif on the Bipyridyl and Acetylide Ligands: Synthesis, Photophysics, and Reverse Saturable Absorption. *Inorg. Chem.* **2014,** *53*, 9516-9530.
65. Neumann, S.; Wenger, O. S., Fundamentally Different Distance Dependences of Electron-Transfer Rates for Low and High Driving Forces. *Inorg. Chem.,* **2019,** *58*, 855-860.
66. Kalyanasundaram, K., Photophysics, photochemistry and solar energy conversion with tris(bipyridyl)ruthenium(II) and its analogues. *Coord. Chem. Rev.,* **1982,** *46*, 159-244.
67. Wallin, S.; Davidsson, J.; Modin, J.; Hammarström, L., Femtosecond Transient Absorption Anisotropy Study on [Ru(bpy)3]2+ and [Ru(bpy)(py)4]2+. Ultrafast Interligand Randomization of the MLCT State. *J. Phys. Chem. A* **2005,** *109*, 4697-4704.
68. Butler, J. M.; George, M. W.; Schoonover, J. R.; Dattelbaum, D. M.; Meyer, T. J., Application of transient infrared and near infrared spectroscopy to transition metal complex excited states and intermediates. *Coord. Chem. Rev.,* **2007,** *251*, 492-514.
69. Yue, Y.; Grusenmeyer, T.; Ma, Z.; Zhang, P.; Schmehl, R. H.; Beratan, D. N.; Rubtsov, I. V., Electron transfer rate modulation in a compact Re(i) donor–acceptor complex. *Dalton Trans.* **2015,** *44*, 8609-8616.
70. Cannizzo, A.; Blanco-Rodríguez, A. M.; El Nahhas, A.; Šebera, J.; Záliš, S.; Vlček, A.; Chergui, M.,

Femtosecond Fluorescence and Intersystem Crossing in Rhenium(I) Carbonyl–Bipyridine Complexes. *J. Am. Chem. Soc.,* **2008,** *130*, 8967-8974.
71. Sutton, J. J.; Li, Y.; Ryu, H. S.; Tay, E. J.; Woo, H. Y.; Gordon, K. C., Fluorination Position: A Study of the Optoelectronic Properties of Two Regioisomers Using Spectroscopic and Computational Techniques. *J. Phys. Chem. A* **2020,** *124*, 7685-7691.
72. Barnsley, J. E.; Shillito, G. E.; Larsen, C. B.; van der Salm, H.; Wang, L. E.; Lucas, N. T.; Gordon, K. C., Benzo[c][1,2,5]thiadiazole Donor–Acceptor Dyes: A Synthetic, Spectroscopic, and Computational Study. *J. Phys. Chem. A* **2016,** *120*, 1853-1866.
73. Sutton, J. J.; Nguyen, T. L.; Woo, H. Y.; Gordon, K. C., Variable-Temperature Resonance Raman Studies to Probe Interchain Ordering for Semiconducting Conjugated Polymers with Different Chain Curvature. *Chem. – Asian J.* **2019,** *14*, 1175-1183.

SYNOPSIS TOC